Coagulation Factor XIII-Binding Aptamer-Modified Nanocomposites for Target Thrombolysis

Chih-Ching Huang [a], Ren-Siang Wu [b], Ming-Lu Lin [c], Yunn-Hwa Ma [c,*]

[a] Department of Bioscience and Biotechnology, National Taiwan Ocean University, Keelung, 202301, Taiwan

[b] Department of Microbiology and Immunology, [c] Department of Physiology and Pharmacology, Graduate Institute of Biomedical Sciences, Chang Gung University, Guishan, Taoyuan 33302, Taiwan

Abstract

Tissue-type plasminogen activator (tPA) is mainly used as a thrombolytic agent for clinical treatments, but its application is limited due to hemorrhagic side effects. Therefore, developing nucleic acid aptamers with high affinity to thrombus for developing thrombus imaging technology and targeted thrombolysis are in high demand. In the present study, aptamer with high affinity toward activated coagulation factor 13 (FXIII) was screened through the phylogenetic evolution of exponentially enriched ligands (SELEX). The factor XIII-binding aptamer was designed to target two main components of thrombus–activated platelets and fibrin. Furthermore, FXIII aptamer-modified gold nanoparticles (FXIII-Au NPs) and FXIII-Au NPs/graphene oxide (FXIII-Au NPs/GO) were shown to bind fibrin clots more efficiently than pristine FXIII aptamer, probably due to the proper orientation of the aptamer on the AuNPs and large surface area of the GO. In addition, further studies suggested that the aptamer-modified nanocomposites were excellent anticoagulants. Our study also introduced the use of carbon nanovesicles (CNVs) for tPA encapsulation, which aimed to protect tPA from enzymatic degradation, prolong its circulation time, and enhance its therapeutic efficacy. Specifically, the nanocarriers were conjugated with FXIII aptamer for clot targeting, concentrating tPA at the required location and minimizing systemic side effects. The CNVs were prepared from amphiphilic carbon dots of sorbitan monooleate (Span 80) using a solvent-injection method. These CNVs were found to encapsulate tPA efficiently and were efficiently conjugated with FXIII aptamer. Transmission electron microscopy revealed spherical CNVs with a size distribution of around 200 nm, suggesting potential for *in vivo* applications. The preserved activity of tPA within the CNVs was confirmed using the S2288 proteolytic activity assay. Further, these nanocomposites effectively dissolved thrombin-induced fibrin clots *in vitro*. Hemolysis assay results demonstrated no hemolytic activity, indicating high biocompatibility of the CNVs.

Specific points

- The FXIIIapt-AuNPs and FXIIIapt-Au NPs/GO exhibit profound binding abilities to fibrin clots and demonstrate excellent anticoagulation activities.
- The conjugation of FXIIIapt on carbon nanovesicles mediated their specific binding to fibrin clots.
- By utilizing FXIII-binding aptamer, specific binding of the nanocomposites to thrombus for anticoagulation therapy and theranostic applications is promising.

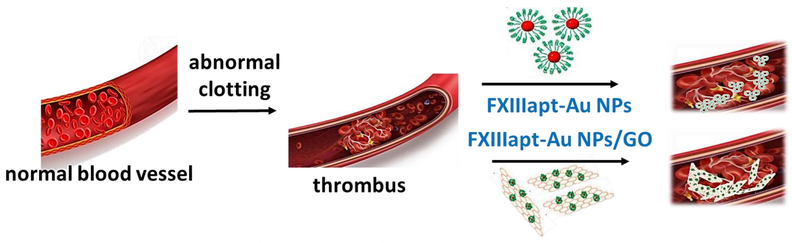

Scheme 1. Schematic illustration of the preparation of FAT2 (FXIIIapt)-modified gold nanoparticles (FXIIIapt-Au NPs) and FXIIIapt-Au NPs-anchored graphene oxide (FXIIIapt-Au NPs/GO) for improving the targeting ability toward thrombus.

Binding of FXIIIapt-FAM, FXIIIapt-Au NPs and FXIIIapt-Au NPs/GO to Fibrin Clots

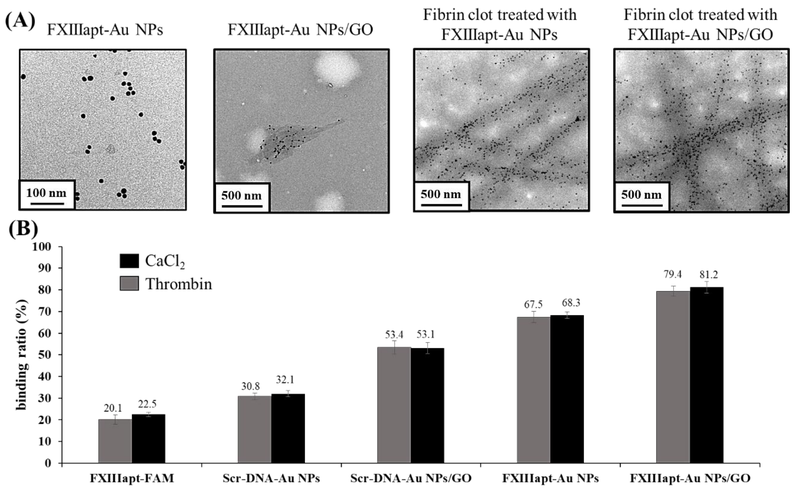

Figure 1. (A) TEM images of FXIIIapt-Au NPs and FXIIIapt-Au NPs/GO binding to fibrin clot. (B) The binding ratio of FXIIIapt-FAM, FXIIIapt-Au NPs and FXIIIapt-Au NPs/GO to fibrin clots. The fibrin clots were formed from human plasma after triggered by thrombin (5 nM) or $CaCl_2$ (8 mM). The FXIIIapt-FAM and FXIIIapt-modified nanoparticles ([FXIIIapt]=100 nM) were incubated with as-formed fibrin clot at room temperature for 30 min. After separating the fibrin clot from unbounded FXIIIapt-FAM, FXIIIapt-Au NPs or FXIIIapt-Au NPs/GO, the binding ratios ([apt]b/[apt]0) were determined through fluorescence (FXIIIapt-FAM) or UV-Vis absorption (FXIIIapt-Au NPs or FXIIIapt-Au NPs/GO) spectroscopic measurements, which [apt]b and [apt]0 is the concentration of as-incubated FXIIIapt (100 nM) and fibrin clot-bound FXIIIapt, respectively. The scramble DNA (scr-DNA) modified-Au NPs (scr-DNA-Au NPs) and -Au NPs/GO (scr-DNA-Au NPs/GO) were conducted as controls. The mean value and standard deviations were determined from three independent experiments.

Preparation and Characterization of Nanocomposites in Binding to Fibrin Clots

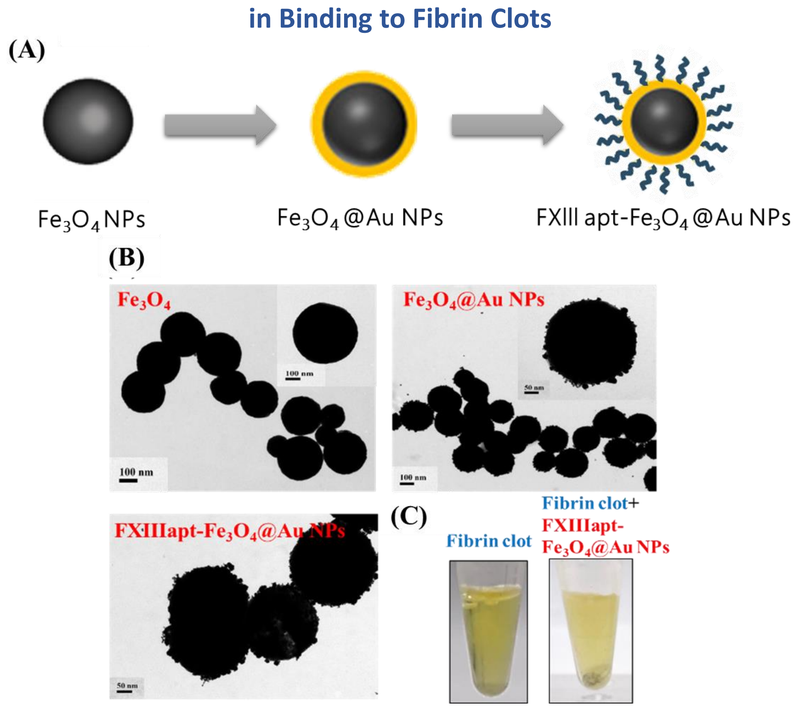

Figure 2. (A) The rationality of preparing FXIIIapt-Fe_3O_4@Au NPs, (B) TEM images of Fe_3O_4 NPs, Fe_3O_4@Au NPs, and FXIIIapt-Fe_3O_4@Au NPs, and (C) the photographs of fibrin clots in the absence and presence of FXIIIapt-Fe_3O_4@Au NPs.

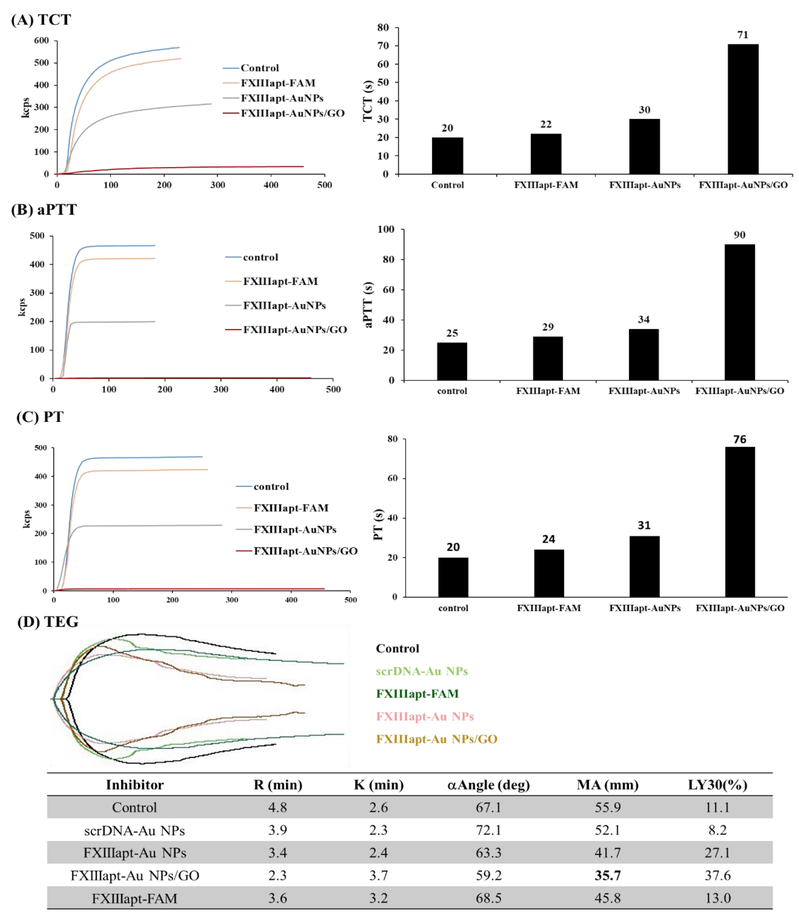

Inhibitor	R (min)	K (min)	αAngle (deg)	MA (mm)	LY30(%)
Control	4.8	2.6	67.1	55.9	11.1
scrDNA-Au NPs	3.9	2.3	72.1	52.1	8.2
FXIIIapt-Au NPs	3.4	2.4	63.3	41.7	27.1
FXIIIapt-Au NPs/GO	2.3	3.7	59.2	**35.7**	37.6
FXIIIapt-FAM	3.6	3.2	68.5	45.8	13.0

Figure 3. A comparison of the anticoagulant activities of free FXIIIapt (i.e., FXIIIapt-FAM), FXIIIapt-Au NPs, and FXIIIapt-Au NPs/GO usung (A) TCT, (B) aPTT, (C) PT, and (D) TEG assays. Error bars represent the standard deviation of four repeated measurements. Light scattering was monitored from samples containing plasma, inhibitor and clotting reagent. The clotting time obtained from the intensity of light scattering as a result of the coagulation process in the presence of inhibitor (control), FXIIIapt, FXIIIapt-Au NPs and FXIIIapt-Au NPs/GO ([FXIIIapt] = 100 nM). The mean value and standard deviations are determined from three independent experiments.

Scheme 2. Schematic representation of (A) the preparation of amphiphilic carbon dots (ACDs) from sorbitan monooleate (Span 80) by an one-step dry-heating method, (B) the preparation of factor XIII (FAT2) aptamer-conjugated, tissue plasminogen activator (tPA)-loaded carbon nanovesicles (FAT2–tPA@CNVs) by a solvent-injection method, and (C) the application of FAT2–tPA@CNVs for targeted thrombolytic therapy *via* intravenous injection.

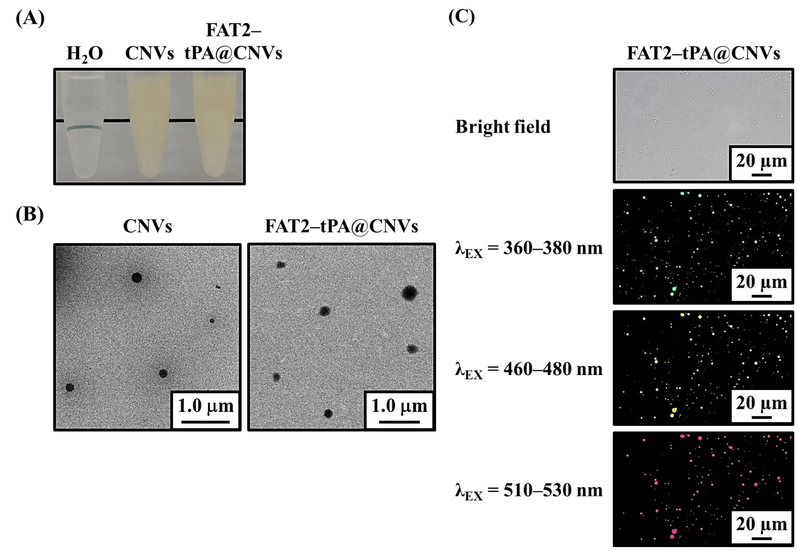

Figure 4. (A) Bright field, (B) transmission electron microscopy (TEM), and (C) fluorescence microscopy images of CNVs and FAT2–tPA@CNVs. The solutions of CNVs and FAT2-tPA@CNVs were prepared in 10 mM phosphate buffer (PB) (pH =7.4).

Fibrinolytic Activities of FAT2–tPA@CNVs

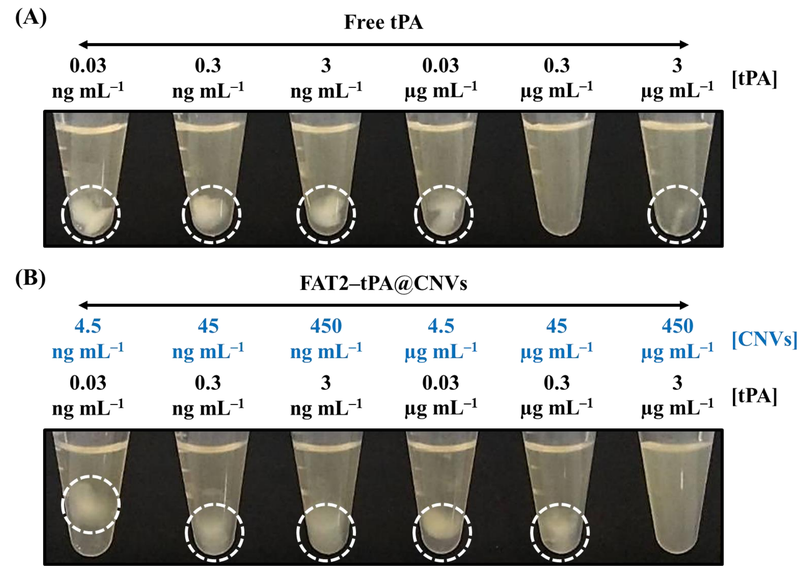

Figure 5. A comparison of fibrinolytic activities of (A) free tPA and (B) FAT2–tPA@CNVs at concentrations ranging from 0.03 ng mL^{-1} to 3 μg mL^{-1} after 8 h of incubation with thrombin-induced fibrin clots of platelet-poor plasma. It was noted that white circle dotted lines indicated the presence of fibrin clots.

Fibrin Clot Binding Assay of FAT2–RB@CNVs

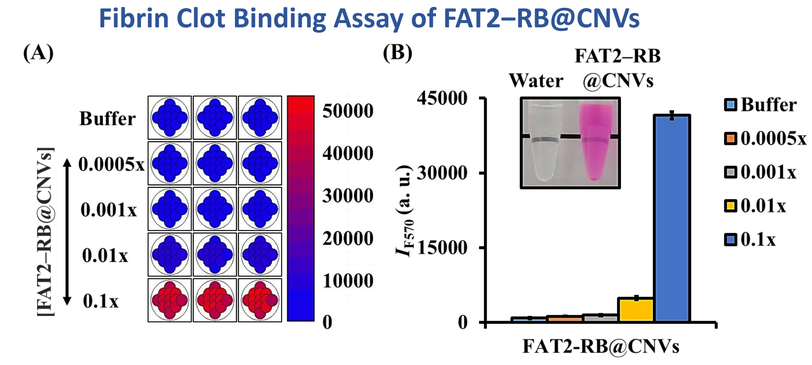

Figure 6. Fibrin clots were prepared from platelet-poor plasma. (A) Fluorescence measurements of the fibrin clots using an area-scanning mode with 13 scanned areas per well and (B) the quantitative results derived from (A). The FAT2-conjugated, rhodamine B-loaded carbon nanovesicles (FAT2–RB@CNVs) were incubated with thrombin-induced PPP fibrin clots for 2 h, followed by three wash steps and fluorescence measurement of the fibrin clots in a microplate reader with an area-scanning mode using an excitation wavelength of 493 nm and an emission wavelength of 517 nm. Insert to (B) demonstrated the appearance of FAT2–RB@CNVs.

Hemolysis Assay of CNVs

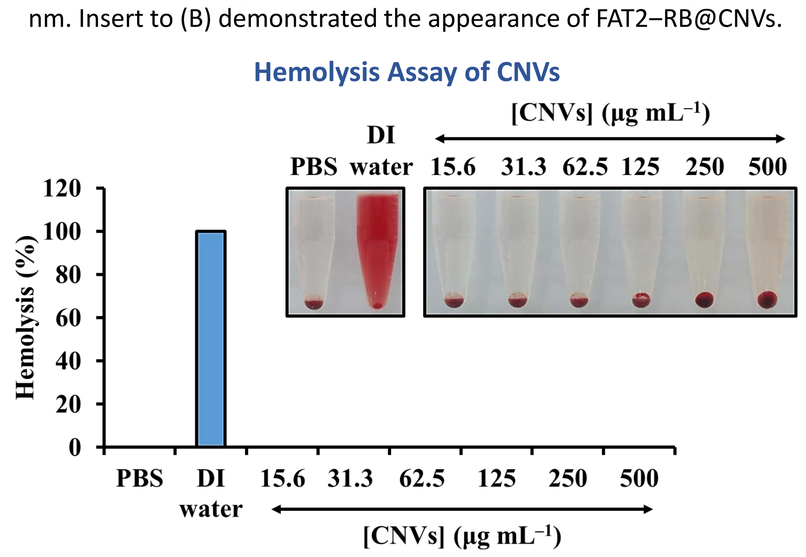

Figure 7. The $CNVs_{span\ 80}$ formulated from amphiphilic carbon dots (ACDs) prepared at (A) 200, (B) 220, and (C) 240°C at concentrations ranging from 15.6–500 μg mL^{-1} were incubated with 4 vol.% human erythrocytes (red blood cells) for 1 h. Subsequently, the mixture of CNVs and erythrocytes was centrifuged at an RCF of 1,000*g* for 10 min to precipitate down the erythrocytes, followed by collection of the supernatants for absorbance measurements at 576 nm to determine the released hemoglobin from lysed erythrocytes.